2024 IEEE 63rd Conference on Decision and Control (CDC)
December 16-19, 2024. MiCo, Milan, Italy

Time-varying State Uncertainty Evaluation of Controlled Robotic Manipulator: Managing Hybrid Uncertainties and Unmeasurable States

1st Dan Bao
Nanjing University of Science and Technology
Nanjing, China
baodan@njust.edu.cn

2nd Jianyong Yao
Nanjing University of Science and Technology
Nanjing, China
yaojianyong@njust.edu.cn

3rd Xiaoling Liang
National University of Singapore
Singapore
elelxl@nus.edu.sg

4th Baolin Hou
Nanjing University of Science and Technology
Nanjing, China
houbl@njust.edu.cn

5th Shuzhi Sam Ge
National University of Singapore
Singapore
samge@nus.edu.sg

***Abstract*—The evaluation of time-varying states furnishes critical data for the control design, reliability analysis, and intelligent decision-making in the operation of robotic manipulators. The presence of limited test conditions along with various uncertainties in the system presents significant challenges to the effectiveness of such evaluations. In response, this study introduces a pioneering approach for state assessment that adeptly manages hybrid uncertainties and states that cannot be directly measured. Within this framework, an extended state observer is integrated into the controller. This observer goes beyond merely monitoring Unmeasurable states; it actively compensates for disturbances, enhancing control precision. By employing Bayesian optimization algorithms and kernel density estimation techniques, the study achieves a nuanced state assessment. The resultant evaluation not only encapsulates interval and probability outcomes but does so in a manner that is seamlessly integrated, offering a detailed portrayal of the dynamic responses and probability distributions at individual time points. This approach substantially enriches our capacity to understand and monitor the complex behaviors of dynamic systems, marking a significant leap forward in the field. Finally, the simulation results significantly validate the algorithm's effectiveness.**

***Index Terms*—Time-varying state evaluation, extended state observer, hybrid uncertainty, Bayesian optimization, kernel density estimation.**

I. Introduction

System time-varying state estimation plays a crucial role in various fields, such as control systems, robotics, and signal processing, where accurate knowledge of the system's internal variables is essential for effective decision-making, reliable analysis, and optimization [1]–[3]. However, this task encounters substantial challenges, first and foremost because of the existence of various uncertainties [4], [5]. These uncertainties manifest as a combination of interval and probability uncertainties, intertwining in a manner that traditional state assessment methodologies struggle to handle adequately. The coexistence of these uncertainties introduces intricacies in modeling and prediction, impacting the accuracy and reliability of state evaluations.

In many practical problems, obtaining the exact values of parameters is challenging, yet establishing upper and lower bounds for these parameters might be feasible. Interval representation allows us to handle uncertainty in a more tolerant manner by considering a range of potential values for the parameters [6], [7]. However, interval representation may introduce information loss as it only offers a broad estimation of the parameter range without providing specific details about the internal distribution of the parameters. Utilizing probability distributions to characterize potential values of parameters enables a more comprehensive understanding of uncertainties [8], [9]. There are different uncertainties in real systems. The mixed uncertainty approach, combining both interval and probability methods, serves as an excellent choice by leveraging the strengths of each [10], [11]. This integrated method offers a broad parameter range estimate in the absence of sufficient data while considering the uncertainty of internal distributions through probability distributions.

Moreover, some states in the system may not be directly measurable due to practical limitations or sensor constraints. This study aims to bridge this gap by introducing an innovative approach to state assessment within controlled dynamic systems [12], [13]. The extended state observer (ESO) can not only observe the measurable state of the system, but also estimate the external disturbance of the system [14]–[16]. In our work, the state information estimated by ESO not only serves as the feedback signal of the controller, but also provides the basis for the dynamic performance evaluation of the system. By providing a mechanism for predicting unmeasurable states, the proposed approach not only enhances the overall observability of the system but also opens avenues for more informed decision-making in the face of uncertainties.

In the process of estimating a system's response or state uncertainty, computational complexity poses a significant challenge, particularly when considering multiple parameters, time-varying state variables, and various uncertainties. While Monte Carlo simulation remains the most commonly used and accurate analytical method, it involves multiple samplings of potential values for system parameters and extensive simulation computations [17], [18]. This can lead to substantial computational overhead, especially when the system model is extensive or simulation costs are high. To enhance efficiency, various methods have been proposed, harnessing the capabilities of parallel computing to meet computational demands. The extreme response surface method was investigated for mechanical dynamic assembly reliability analysis [19]. A polynomial chaos expansion method was proposed to estimate the dynamic response bounds of nonlinear systems [20]. The radial basis functions were used to analyze static response considering interval uncertainty [21]. A recurrent neural network was proposed to predict the dynamic response of robotic systems [22]. However, constructing surrogate models also requires an ample amount of sample data. The above study estimated the range of system responses without delving into the distribution within that interval. Further investigation and analysis are required to understand the specific distribution characteristics of system responses within the mentioned range.

The main contributions are highlighted as follows: (i) Introduces a state observer within the controller, enabling the prediction of traditionally unmeasurable states and enhancing the system's overall observability. (ii) Bayesian optimization and kernel density estimation provide a practical and effective solution for real-time state evaluation in uncertain environments.

The paper is organized as follows. Section II delineates the research problems addressed in this paper. Subsequently, Section III details the design of a feedback controller tailored to the system's characteristics. In Section IV, the system state boundaries are estimated using Bayesian optimization, while the KDE method is employed to estimate the distribution of the system state at specific time points. A simulation example is presented to validate the efficacy of the proposed method in Section V. Section VI offers a comprehensive summary of the entire paper.

II. Problem description

Consider the following dynamic equation for n degree of freedom (n-DOF) robotic systems:

$$\boldsymbol{M}(\boldsymbol{q})\ddot{\boldsymbol{q}} + \boldsymbol{C}(\boldsymbol{q},\dot{\boldsymbol{q}})\dot{\boldsymbol{q}} + \boldsymbol{G}(\boldsymbol{q}) + \boldsymbol{T_f} + \boldsymbol{\tau_d} = \boldsymbol{\tau} \tag{1}$$

where, $\boldsymbol{q} \in R^n$, $\dot{\boldsymbol{q}} \in R^n$, and $\ddot{\boldsymbol{q}} \in R^n$ are position, velocity, and acceleration vectors, respectively; $\boldsymbol{M}(\boldsymbol{q})$ denotes symmetric and positive definite matrix of inertia; $\boldsymbol{C}(\boldsymbol{q},\dot{\boldsymbol{q}})$ denotes the Coriolis and Centrifugal term matrix; $\boldsymbol{G}(\boldsymbol{q})$ denotes the gravity term; $\boldsymbol{T_f}$ is the friction vector; $\boldsymbol{\tau_d}$ represents unmodeled functions and external disturbances, $\boldsymbol{\tau}$ is the control input.

Due to machining errors, assembly errors, environmental changes and other factors, the system has various uncertain parameters. Define the uncertain parameters as $\boldsymbol{u} = [u_1, u_2, ..., u_n]^T$. It is difficult to obtain the distribution law of some parameters, but it is possible to know the variation interval. These parameters are expressed in the form of uniformly distributed intervals, $u_i \in {u_i}^I = [\underline{u}_i, \overline{u}_i]$. The superscript I represents the interval, $\underline{u}_i$ and $\overline{u}_i$ are the lower boundary and upper boundary of the interval.

If a uncertainty parameter u_j following a normal distribution with a mean μ and a standard deviation σ, denoted as $u_j \sim \mathcal{N}(\mu, \sigma^2)$. In theory, the normal distribution is defined over the entire real number line and does not have boundaries. However, in practical situations, variables may have physical or practical constraints, leading to bounded distributions. For instance, certain measured quantities cannot be negative, or they may have an upper limit. In such cases, a truncated normal distribution is considered. A truncated normal distribution is a normal distribution that is restricted to a specific interval. The variable u_j is truncated within the interval $[\underline{u}_j, \overline{u}_j]$, its probability density function can be expressed as:

$$f(u_j;\mu,\sigma,\underline{u}_j,\overline{u}_j) = \begin{cases} \frac{1}{\omega}\phi\left(\frac{u_j-\mu}{\sigma}\right), & \text{if } \underline{u}_j \le u_j \le \overline{u}_j \\ 0, & \text{otherwise} \end{cases} \tag{2}$$

where ϕ is the probability density function of the standard normal distribution, and ω is the normalization factor ensuring that the probability density function integrates to 1 within the specified interval. For a truncated normal distribution, the normalization factor is usually calculated by integrating the probability density function over a given interval. In this context, the normal distribution has zero probability density outside the interval $[\underline{u}_j, \overline{u}_j]$, and within the interval, it follows the standard normal distribution pattern, albeit scaled and shifted. Using this approach helps convey the information about the distribution parameters in a clear and precise manner.

Under the influence of uncertain parameters $\boldsymbol{u}$, the state of the system is within ranges and there is a distribution feature within that range. In a motion time, the system dynamic states can be presented as Fig. 1.

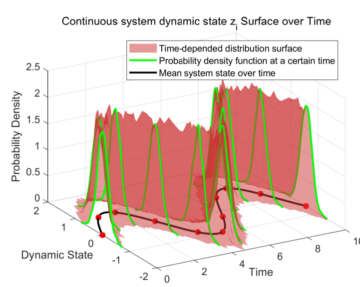

Fig. 1: Dynamic state uncertainty over motion time.

In the process of system dynamic state evaluation, one challenge is how to get the state of the system. In engineering practice, some system states can be measured by sensors, while some states are difficult to obtain due to structural complexity, environmental badness and cost problems. To deal with this problem, a state observer is introduced into the control system. The output of the state observer can provide more data support for system dynamic performance evaluation. Another challenge is how to calculate the interval and distribution of states.

The research content and research process block diagram are shown in Fig. 2, which mainly consists two parts. The first part aims to design a controller, and another part is to calculate the uncertain states with Bayesian optimization method and kernel density estimator.

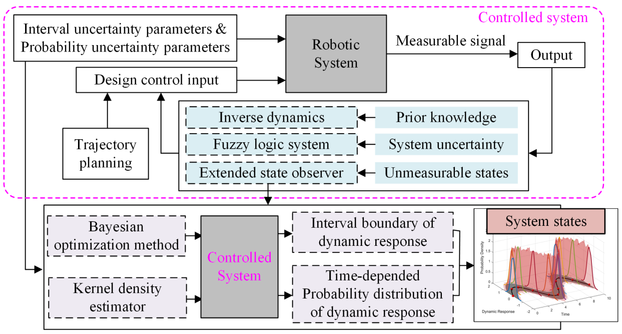

Fig. 2: Block diagram of the research content.

III. Feedback adaptive controller design

In this section a feedback adaptive control method is proposed for the nonlinear robotic manipulator, which involves three characteristics as shown in Fig. 1. Firstly, it uses the known information of the system, secondly, the unknown nonlinear terms are compensated by means of data-driven method, finally, an extended state observer is introduced to monitor system states and deal with disturbances.

Before designing the controller, some assumptions are provided here.

Assumption 1: The function $\boldsymbol{f}(\boldsymbol{x_1}, \boldsymbol{x_2})$ is locally Lipschitz continuous functions with respect to $\boldsymbol{x_2}$ in its practical range.

According to Assumption 1, there exists a constant c_1 that satisfies the following conditions

$$\left|\tilde{\boldsymbol{f}}\right| = \left|\boldsymbol{f}(\boldsymbol{x_1}, \boldsymbol{x_2}) - \boldsymbol{f}(\boldsymbol{x_1}, \hat{\boldsymbol{x}}_2)\right| \leq c_1 \left|\tilde{\boldsymbol{x}}_2\right| \tag{3}$$

Based on the center of the interval uncertainty parameter $\boldsymbol{u}^c = (\underline{\boldsymbol{u}} + \overline{\boldsymbol{u}})/2$ or the mean value of the probabilistic uncertainty parameter, the nominal values of the matrix $\boldsymbol{M}$, $\boldsymbol{C}$ and $\boldsymbol{G}$ can be calculated. This nominal value can provide a part of the system prior information for the controller design. The matrix $\boldsymbol{M}$, $\boldsymbol{C}$, and vector $\boldsymbol{G}$ can be formulated as $\boldsymbol{M} = \boldsymbol{M_0} + \boldsymbol{\delta_M}$, $\boldsymbol{C} = \boldsymbol{C_0} + \boldsymbol{\delta_C}$, and $\boldsymbol{G} = \boldsymbol{G_0} + \boldsymbol{\delta_G}$. Parameters $\boldsymbol{\delta_M}$, $\boldsymbol{\delta_C}$, and $\boldsymbol{\delta_G}$ are unknown terms, and parameters $\boldsymbol{M_0}$, $\boldsymbol{C_0}$, and $\boldsymbol{G_0}$ are nominal terms.

Define system states as $\boldsymbol{x}_1 = \boldsymbol{q} \in R^n$ and $\boldsymbol{x}_2 = \dot{\boldsymbol{q}} \in R^n$. Then, the dynamic model can be represented in the state space form as

$$\begin{cases} \dot{\boldsymbol{x}}_1 = \boldsymbol{x_2} \\ \dot{\boldsymbol{x}}_2 = \boldsymbol{H_0}\boldsymbol{\tau} + \boldsymbol{f}(\boldsymbol{x}_1, \boldsymbol{x}_2) + \boldsymbol{H_0}\boldsymbol{\varphi} + \boldsymbol{\tau_{d0}} \\ \boldsymbol{y} = \boldsymbol{x_1} \end{cases} \tag{4}$$

where

$$\begin{cases} \boldsymbol{H_0} = (\boldsymbol{M_0})^{-1} \\ \boldsymbol{f}(\boldsymbol{x}_1, \boldsymbol{x}_2) = (\boldsymbol{M_0})^{-1}(-\boldsymbol{C_0}\boldsymbol{x}_2 - \boldsymbol{G_0}) \\ \boldsymbol{\varphi} = -\boldsymbol{\delta_M}\dot{\boldsymbol{x}}_2 - \boldsymbol{\delta_C}\boldsymbol{x}_2 - \boldsymbol{\delta_G} \\ \boldsymbol{\tau_{d0}} = (\boldsymbol{M_0})^{-1}\boldsymbol{\tau_d} \end{cases} \tag{5}$$

In the above equation, the terms $\boldsymbol{H_0}$ and $\boldsymbol{f}(\boldsymbol{x}_1, \boldsymbol{x}_2)$ can be calculated. Fuzzy logic system (FLS) is adopted to approximate the unknown function $\boldsymbol{\varphi} \in R^n$, which can be expressed as follows.

$$\boldsymbol{\varphi}(\bar{\boldsymbol{x}}) = \boldsymbol{\theta}^T \boldsymbol{\phi}(\bar{\boldsymbol{x}}) + \boldsymbol{\varepsilon} \tag{6}$$

where $\bar{\boldsymbol{x}}$ is the input of the FLS, $\boldsymbol{\theta} = \mathrm{diag}(\boldsymbol{\theta_1}, \boldsymbol{\theta_2}, ..., \boldsymbol{\theta_n}) \in R^{mn \times n}$ is a weight vector of FLSs, $\boldsymbol{\theta_i} \in R^m$ is the weight vector of every FLS, $\boldsymbol{\phi}(\bar{\boldsymbol{x}}) = [\boldsymbol{\phi}(\bar{\boldsymbol{x}}_1), \boldsymbol{\phi}(\bar{\boldsymbol{x}}_2), ..., \boldsymbol{\phi}(\bar{\boldsymbol{x}}_n)]^T \in R^{mn \times 1}$ is the basis function vector, $\boldsymbol{\varepsilon} \in R^n$ is the approximation error. The optimal weight is given by

$$\boldsymbol{\theta}^* = \arg\min \left[\sup_{\boldsymbol{x} \in \Omega_x} \left|\boldsymbol{\varphi}(\boldsymbol{x}\,|\boldsymbol{\theta}) - \boldsymbol{\varphi}(\boldsymbol{x})\right| \right] \tag{7}$$

The estimation errors of FLSs and the lumped disturbance in (6) are expended to a state $\boldsymbol{x_3} \in R^n$, which is formulated as $\boldsymbol{x_3} = \boldsymbol{H_0}\boldsymbol{\varepsilon} + \boldsymbol{\tau_{d0}}$.

Assumption 3: The derivative $\boldsymbol{\delta} \in R^n$ of the state $\boldsymbol{x_3}$ is to be bounded, i.e., $\|\boldsymbol{\delta}(\boldsymbol{t})\|_\infty \leq \bar{\delta}$, where $\bar{\delta}$ is a unknown positive constant.

Inspired by Ref. [16], an nonlinear ESO is designed as:

$$\begin{cases} \dot{\hat{\boldsymbol{x}}}_1 = \hat{\boldsymbol{x}}_2 + \kappa_1 \boldsymbol{g}(\tilde{\boldsymbol{x}}_1, \lambda_1) \\ \dot{\hat{\boldsymbol{x}}}_2 = \boldsymbol{H_0}\boldsymbol{\tau} + \boldsymbol{f}(\boldsymbol{x}_1, \hat{\boldsymbol{x}}_2) + \boldsymbol{H_0}\hat{\boldsymbol{\theta}}^T \boldsymbol{\phi} + \hat{\boldsymbol{x}}_3(t) + \kappa_2 \boldsymbol{g}(\tilde{\boldsymbol{x}}_1, \lambda_2) \\ \dot{\hat{\boldsymbol{x}}}_3 = \kappa_3 \boldsymbol{g}(\tilde{\boldsymbol{x}}_1, \lambda_3) \\ \boldsymbol{y} = \boldsymbol{x}_1 \end{cases} \tag{8}$$

where κ_1, κ_2, and κ_3 are design parameters. In order to reduce adjustable parameters in the controller, there are the following parameter settings: $\kappa_1 = 3\kappa_0$, $\kappa_2 = 3{\kappa_0}^2$, and $\kappa_3 = {\kappa_0}^3$. In addition, $\lambda_1 = \lambda_2 = \lambda_3 = \lambda$. The term $\hat{\boldsymbol{x}}_2$ is the estimation of $\boldsymbol{x_2}$ and the term $\hat{\boldsymbol{x}}_3$ is the estimation of $\boldsymbol{x_3}$. The parameter $\hat{\boldsymbol{\theta}}$ is the estimated value of the optimal value $\boldsymbol{\theta}^*$. The nonlinear function $\boldsymbol{g} \in R^n$ is defined as follows

$$\boldsymbol{g}(\tilde{\boldsymbol{x}}_1, \lambda) = \begin{cases} \tilde{\boldsymbol{x}}_1 + |\tilde{\boldsymbol{x}}_1|^\lambda \mathrm{sign}(\tilde{\boldsymbol{x}}_1), & \|\tilde{\boldsymbol{x}}_1\|_\infty > \varepsilon_x \\ \tilde{\boldsymbol{x}}_1, & \text{otherwise} \end{cases} \tag{9}$$

where $0 < \lambda < 1$ is a constant, $\mathrm{sign}(\cdot)$ is a symbolic function.

Define the tracking errors as follows:

$$\begin{aligned} \boldsymbol{e_1} &= \boldsymbol{x_1} - \boldsymbol{x_d} \\ \boldsymbol{e_2} &= \boldsymbol{x_2} - \boldsymbol{\alpha_1} \end{aligned} \tag{10}$$

where $\boldsymbol{x_d}$ is the desire trajectory. The virtual control $\boldsymbol{\alpha}_1$ is designed as

$$\boldsymbol{\alpha_1} = -\boldsymbol{K_1}\boldsymbol{e_1} + \dot{\boldsymbol{x}}_d \tag{11}$$

where $\boldsymbol{K_1} \in R^{n \times n}$ is a designed positive definite matrix, $\dot{\boldsymbol{x}}_d$ is the desire velocity.

The control input is introduced as

$$\begin{aligned} \boldsymbol{\tau} = &-\boldsymbol{e_1} - \boldsymbol{K_2}\hat{\boldsymbol{e}}_2 + \boldsymbol{C_0}(\boldsymbol{x_1}, \hat{\boldsymbol{x}}_2)\boldsymbol{\alpha_1} + \boldsymbol{G_0}(\boldsymbol{x_1}) \\ &+ \boldsymbol{M_0}(\dot{\boldsymbol{\alpha}}_1 - \hat{\boldsymbol{x}}_3) - {\boldsymbol{M_0}}^{-1}\hat{\boldsymbol{\theta}}^T \boldsymbol{\phi} \end{aligned} \tag{12}$$

where $\boldsymbol{K_2} \in R^{n\times n}$ is a designed positive definite matrix, $\hat{\boldsymbol{e}}_2 = \hat{\boldsymbol{x}}_2 - \boldsymbol{\alpha_1}$, $\dot{\boldsymbol{\alpha}}_1 = -\boldsymbol{K_1}\hat{\boldsymbol{x}}_2 + \ddot{\boldsymbol{x}}_d$.

Furthermore, the adaptive law of weight vector in FLS is proposed as :

$$\dot{\hat{\boldsymbol{\theta}}}_i = \boldsymbol{\Gamma_i}\left(\eta_i\boldsymbol{\phi_i} + \gamma_i\hat{\boldsymbol{\theta}}_i\right) \tag{13}$$

where $\boldsymbol{\Gamma_i} = \boldsymbol{\Gamma_i}^{-1}$ is a positive definite matrix, $\boldsymbol{\eta} = [\eta_1, \eta_2, ..., \eta_n]^T$, and γ_i is positive designed parameters.

Theorem 1: Considering the extended state observer (8) designed for the nonlinear system (1), the state estimation errors are bounded in finite time with appropriate constant parameters κ_1, κ_2, and κ_3.

Theorem 2: For the nonlinear robotic system (1) subject to uncertainties and disturbances, the FLSs are designed as (6) and (7). The adaptation laws of FLS weight vector $\boldsymbol{\theta_i}$ are chosen as (13). Under the adaptive feedback control scheme proposed as (12), the semiglobal stability of the closed-loop system is guaranteed.

Considering the length of the paper, the proofs of Theorem 1 and Theorem 2 are omitted.

IV. UNCERTAINTY EVALUATION OF DYNAMIC SYSTEM STATS

A. Interval Calculation based on BO Algorithm

The interval boundary of a dynamic state is essentially the extreme value of the solution of a dynamic equation at every integral. In general, the Monte Carlo (MC) method is the simplest, most commonly used, and most accurate method. Due to its high computational cost, it is usually only used to generate reference solutions. Define the system state vector as $\boldsymbol{z(t)} = [\boldsymbol{z_1}, \boldsymbol{z_2}] = [\boldsymbol{x}_1, \boldsymbol{x}_2]$. In order to obtain the dynamic state boundary quickly and accurately, this paper presents a method based on Bayesian optimization (BO) to obtain the system state boundary. Uncertainty parameters $\boldsymbol{u}$ is the design parameter to be optimized, and the minimization or maximization of state $\boldsymbol{z(t)}$ is the optimization goal.

The time range $t \in [t_0, t_e]$ is discretized into a set of interpolation points $(t_0, t_1, ..., t_k, ..., t_e)$ and then the solution at each time node is computed in turn. Fig. 3 shows the procedure for calculating the dynamic boundary of state $\boldsymbol{z_1}$.

Method BO is a probabilistic model-based optimization technique that aims to efficiently find the maximum or minimum of an objective function. It combines a probabilistic surrogate model with an acquisition function to guide the search for optimal solutions [23], [24]. This process can be described in three steps.

Step 1: A Gaussian process model is constructed according to the current sample points at each time.

Step 2: Based on joint probability density function, the probability density function, and Bayesian theory $P(AB) = P(A) * P(B\,|A)$, calculate the posterior probability distribution.

Step 3: Design an acquisition function. Then, Maximizing or minimizing the acquisition function can obtain the next sampling point. The response of the new sample points is then calculated and the sample set is updated.

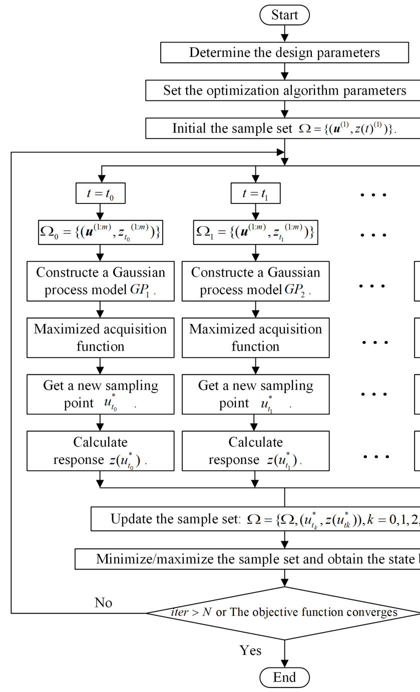

Fig. 3: The boundary calculation process for state over time $[t_0, t_e]$.

Remark 1: It needs to be pointed out that Gaussian processes at all times share a sample set, and new sample points obtained by Bayesian optimization at each time are added to the total sample set.

Remark 2: In Step 3, the problem of maximizing or minimizing the acquisition function is solved by particle swarm optimization algorithm [25].

B. Time-depended Probability distribution of system states

Kernel Density Estimation (KDE) is a non-parametric statistical technique used to estimate the probability density function of a random variable. It works by placing a kernel (a smooth, symmetric, and non-negative function) at each data point and summing them to create a continuous density estimate. The KDE method provides a flexible way to visualize the underlying distribution of data, helping to identify patterns, modes, and overall shape.

The definition of kernel density estimation is provided as follows

$$p(x) = \frac{1}{n\sigma}\sum_{i=1}^{n} K\left(\frac{x - x_i}{\sigma}\right) \tag{14}$$

where $\{x_i\}_{i=1}^n$ is a given set of data points, n is the number of points, K denotes the kernel function, σ is a bandwidth parameter. The common kernel functions include uniform kernel, Quadric kernel, and Epanechnikov kernel. Epanechnikov kernel functions have some advantages over other kernel functions, such as their relatively small bandwidth and therefore low sensitivity to noise. The expression of the Epanechnikov kernel function is as follows:

$$K(z) = \frac{3}{4}(1 - z^2), \text{for } |z| \leq 1 \tag{15}$$

Here, z is the standardized variable representing the relative distance from a particular observation point. The Epanechnikov kernel has the shape of a smooth parabola with a width of 2, exhibiting non-zero values within its core region $[-1, 1]$ and zero values outside the core. This configuration ensures that data points farther away from the observation point contribute less to the probability density estimation during the process, providing a certain level of smoothing effect.

In order to evaluate the time-depended probability distribution of system states, probability distribution at every time point is calculated. This detailed computation allows for a nuanced understanding of how the likelihood of various system states changes over time, providing insights into the system's dynamic behavior under different conditions. The approach is particularly useful in systems characterized by inherent uncertainties or those subjected to external perturbations, as it provides a framework for quantifying the impact of such variables on the system's performance over time. It facilitates the identification of potential risks, thereby contributing to more robust and reliable system design and operation.

V. Simulation Results

In the simulation section of our research, we explored the capability of our proposed approach to assess time-varying states in the context of controlled robotic manipulators. The results of these simulations provided a nuanced understanding of how the system's dynamic responses and probability distributions evolve over time, illustrating the potential of our innovative approach to significantly improve the precision of state assessment under conditions of hybrid uncertainties.

In order to demonstrate the validity of the present method, a simulation example on a two-DOF robot manipulator is performed and analyzed. The dynamic model of the system is described as equ.(1). The terms $\boldsymbol{M}$, $\boldsymbol{C}$, and $\boldsymbol{G}$ are calculated as Ref. [22]. The friction force is modeled by Gauss exponent model which takes Stribeck phenomenon into account

$$\boldsymbol{T_f} = \frac{2}{\pi}\arctan(A_s\dot{\boldsymbol{q}})\left[\boldsymbol{M_{fc}} + (\boldsymbol{M_{fs}} - \boldsymbol{M_{fc}})e^{-(\dot{\boldsymbol{q}}/\dot{\boldsymbol{q}}_s)^2}\right] \tag{16}$$

where $\boldsymbol{M_{fc}}$ is Coulomb friction, $\boldsymbol{M_{fs}}$ is the maximum static friction, A_s is the shape correction factor, $\dot{\boldsymbol{q}}_s$ is the Stribeck velocity. These four parameters are regarded as interval uncertainty parameters. In addition, the external disturbance is modeled as $\boldsymbol{\tau_d} = [\sin(t)\cos(t); \sin(2t)\cos(t)]$. The desired trajectory is given by $x_{di} = \sin(2\pi t), i = 1, 2$. The initial conditions for the simulation study are selected as $\boldsymbol{x_1} = [0; 0]$, $\boldsymbol{x_2} = [2\pi; 2\pi]$.

The uncertain parameters in the system are denoted as $\boldsymbol{u} = [m_1, m_2, l_1, l_2, A_s, M_{fc}, M_{fs}, q_s]^T$, and their characteristic condition are provided in Table I. The structural parameters m_1, m_2, l_1, and l_2 of the system follow a truncated normal distribution, while the parameters A_s, M_{fc}, M_{fs}, and $\dot{q}_s$ in the friction model are treated as interval uniformly distributed parameters. In the simulation, the user input parameters are set as $\kappa_0 = 15$, $\lambda = 0.5$, $\boldsymbol{K_1} = \text{diag}(60, 60)$, $\boldsymbol{K_2} = \text{diag}(60, 60)$, $\boldsymbol{\Gamma_i} = \text{diag}(5, 5)$, $\gamma_i = 3$.

TABLE I: Characteristics of uncertain variables

Uncertain variable	Uncertainty type	lower bound	upper bound	mean value	variance value
m_1	interval-probability	1.2	1.4	1.3	0.06
m_2	interval-probability	1.4	1.6	1.5	0.05
l_1	interval-probability	0.40	0.44	0.42	0.01
l_2	interval-probability	0.32	0.36	0.33	0.01
A_s	interval	90	120	-	-
M_{fc}	interval	2	6	-	-
M_{fs}	interval	8	12	-	-
$\dot{q}_s$	interval	0.8	1.2	-	-

The simulation results are analyzed below to illustrate the effectiveness of the proposed method. Initially, the tracking error boundary is estimated using the BO algorithm flow depicted in Fig. 3. The simulation spans from time 0 to 3 seconds. The tracking error interval is computed every 0.05 seconds throughout the 3-second simulation, and the corresponding boundaries are determined. Fig. 4 presents the simulation results for state tracking errors, including position tracking errors and velocity tracking errors. Additionally, results obtained using the Monte Carlo (MC) method are provided for comparison, which based on 10000 simulations. It can be seen from the figures that the boundary obtained through BO is almost the same as the boundary obtained through MC.

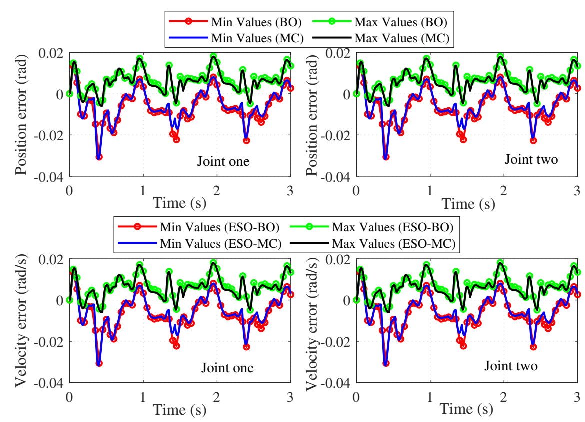

Fig. 4: Comparison of interval boundary prediction between method BO and method MC.

In addition, the state output distribution at a specific time point is estimated by KDE method. The results obtained by MC method are used as comparison group. Fig. 5 shows the distribution of the state tracking error of two degrees of freedom at three time points $t = 1.0$ s, 2.0 s, 3.0 s, respectively. We can observe that the PDF curves obtained by the two methods almost coincide.

VI. Conclusion

This paper introduces a novel approach for evaluating the uncertainty in system states, incorporating the effects of both interval and probability uncertainties while addressing scenarios where certain states are unmeasurable. The proposed state observer design enhances overall system observability, predicting traditionally unmeasurable states. Coupled

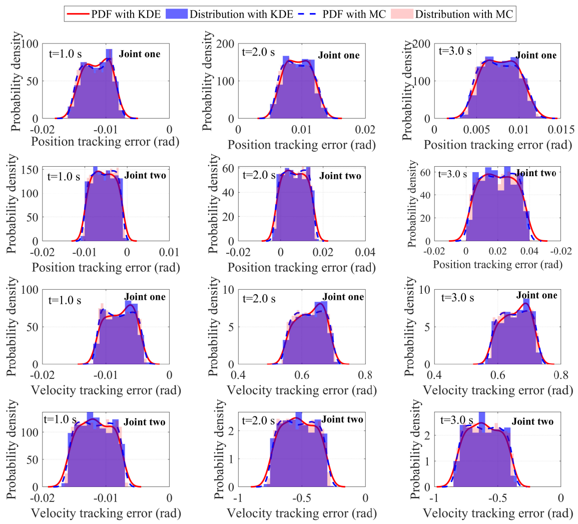

Fig. 5: Comparison of distribution prediction between KDE method and MC method.

interval-probability analysis provides a comprehensive evaluation of time-dependent state variations. The utilization of advanced techniques, including Bayesian optimization and kernel density estimation, improves computational efficiency for decision-making in uncertain environments. Simulation results affirm the effectiveness of the proposed methodologies, offering accurate state predictions and reliable information support. These contributions advance dynamic system analysis, providing valuable insights for developing robust systems capable of handling complex and uncertain dynamics across various applications in engineering and beyond.

Acknowledgments

This research is supported by the National Research Foundation Singapore under its AI Singapore Programme (Award Number: [AISG2-GC-2023-007]), also supported by Enabling Future Systems for Offshore Wind Resources (EN-FORCE) programme supported by A*STAR under its RIE 2025 Industry Alignment Fund (Grant No. M23M4a0067), and the National Natural Science Foundation of China (Grand No. 52405115).

References

[1] X. Liang, D. Bao, and S. S. Ge, "Modeling of neuro-fuzzy system with optimization algorithm as a support in system boundary capability online assessment," *IEEE Transactions on Circuits and Systems II: Express Briefs*, vol. 70, no. 8, pp. 2974–2978, 2023.

[2] Y. Tian, T. Floquet, and W. Perruquetti, "Fast state estimation in linear time-varying systems: an algebraic approach," in *2008 47th IEEE Conference on Decision and Control*. IEEE, 2008, pp. 2539–2544.

[3] X. Kong and G. Yang, "Secure state estimation for train-to-train communication systems: A neural network-aided robust ekf approach," *IEEE Transactions on Industrial Electronics*, 2024.

[4] T. D. Barfoot, *State estimation for robotics*. Cambridge University Press, 2024.

[5] C. Zhang, J. Qin, C. Yan, Y. Shi, Y. Wang, and M. Li, "Towards invariant extended kalman filter-based resilient distributed state estimation for moving robots over mobile sensor networks under deception attacks," *Automatica*, vol. 159, p. 111408, 2024.

[6] C. Jiang, R. G. Bi, G. Y. Lu, and X. Han, "Structural reliability analysis using non-probabilistic convex model," *Computer Methods in Applied Mechanics and Engineering*, vol. 254, pp. 83–98, 2013.

[7] D. Zhang, M. Van, S. Mcllvanna, Y. Sun, and S. McLoone, "Adaptive safety-critical control with uncertainty estimation for human–robot collaboration," *IEEE Transactions on Automation Science and Engineering*, 2023.

[8] D. Zhang, Z. Peng, G. Ning, and X. Han, "Positioning accuracy reliability of industrial robots through probability and evidence theories," *Journal of Mechanical Design*, vol. 143, no. 1, 2021.

[9] S. S. Rao and P. K. Bhatti, "Probabilistic approach to manipulator kinematics and dynamics," *Reliability Engineering System Safety*, vol. 72, no. 1, pp. 47–58, 2001. [Online]. Available: https://www.sciencedirect.com/science/article/pii/S095183200000106X

[10] C. Zeng, Z. Qiu, F. Zhang, and X. Zhang, "Error modelling and motion reliability analysis of a multi-dof redundant parallel mechanism with hybrid uncertainties," *Reliability Engineering System Safety*, vol. 235, 2023.

[11] D. Zhang, S. Liu, J. Wu, Y. Wu, and J. Liu, "An active learning hybrid reliability method for positioning accuracy of industrial robots," *Journal of Mechanical Science and Technology*, vol. 34, no. 8, pp. 3363–3372, 2020.

[12] G. Yang, J. Yao, and N. Ullah, "Neuroadaptive control of saturated nonlinear systems with disturbance compensation," *ISA Transactions*, vol. 122, pp. 49–62, 2022.

[13] C. N. Hadjicostis, S. Lafortune, F. Lin, and R. Su, "Cybersecurity and supervisory control: A tutorial on robust state estimation, attack synthesis, and resilient control," in *2022 IEEE 61st Conference on Decision and Control (CDC)*. IEEE, 2022, pp. 3020–3040.

[14] Z. Zhao and B. Guo, "A novel extended state observer for output tracking of mimo systems with mismatched uncertainty," *IEEE Transactions on Automatic Control*, vol. 63, no. 1, pp. 211–218, 2018.

[15] D. T. Tran, M. Jin, and K. K. Ahn, "Nonlinear extended state observer based on output feedback control for a manipulator with time-varying output constraints and external disturbance," *IEEE Access*, vol. 7, pp. 156 860–156 870, 2019.

[16] M. Chen and S. S. Ge, "Adaptive neural output feedback control of uncertain nonlinear systems with unknown hysteresis using disturbance observer," *IEEE Transactions on Industrial Electronics*, vol. 62, no. 12, pp. 7706–7716, 2015.

[17] J. C. O. Pena and L. A. Tôrres, "Uncertainty in the estimation of end-effector acceleration and angular velocity for robotic manipulators," in *2016 XIII Latin American Robotics Symposium and IV Brazilian Robotics Symposium (LARS/SBR)*, 2016, pp. 281–286.

[18] V. T. Aghaei, A. Ağababaoğlu, S. Yıldırım, and A. Onat, "A real-world application of markov chain monte carlo method for bayesian trajectory control of a robotic manipulator," *ISA transactions*, vol. 125, pp. 580–590, 2022.

[19] C. Fei and G. Bai, "Distributed collaborative extremum response surface method for mechanical dynamic assembly reliability analysis," *Journal of Central South University*, vol. 20, no. 9, pp. 2414–2422, 2013.

[20] L. Wang, Z. Chen, and G. Yang, "A polynomial chaos expansion approach for nonlinear dynamic systems with interval uncertainty," *Nonlinear Dynamics*, vol. 101, no. 4, pp. 2489–2508, 2020.

[21] Y. Liu, X. Wang, and L. Wang, "Interval uncertainty analysis for static response of structures using radial basis functions," *Applied Mathematical Modelling*, vol. 69, pp. 425–440, 2019.

[22] D. Bao, X. Liang, S. S. Ge, and B. Hou, "A deep motion reliability scheme for robotic operations," *Mechanism and Machine Theory*, vol. 183, p. 105280, 2023. [Online]. Available: https://www.sciencedirect.com/science/article/pii/S0094114X2300054X

[23] E. d. Castillo and M. S. Reis, "Bayesian predictive optimization of multiple and profile response systems in the process industry: A review and extensions," *Chemometrics and Intelligent Laboratory Systems*, vol. 206, 2020.

[24] D. Bao, X. Liang, S. S. Ge, and B. Hou, "Adaptive neural trajectory tracking control for n-dof robotic manipulators with state constraints," *IEEE Transactions on Industrial Informatics*, 2022.

[25] D. Freitas, L. G. Lopes, and F. Morgado-Dias, "Particle swarm optimisation: A historical review up to the current developments," *Entropy (Basel)*, vol. 22, no. 3, 2020.